Microarray-Based Identification of *Tenascin C* and *Tenascin XB*, Genes Possibly Involved in Tumorigenesis Associated with Neurofibromatosis Type 1

Pascale Lévy,[1] Hugues Ripoche,[2] Ingrid Laurendeau,[1] Vladimir Lazar,[3] Nicolas Ortonne,[4] Béatrice Parfait,[1] Karen Leroy,[4] Janine Wechsler,[4] Isabelle Salmon,[6] Pierre Wolkenstein,[5] Philippe Dessen,[2] Michel Vidaud,[1] Dominique Vidaud,[1] and Ivan Bièche[1,7]

Abstract

Purpose: Neurofibromatosis type 1 (NF1) is an autosomal dominant disorder with a complex variety of clinical manifestations. The hallmark of NF1 is the onset of heterogeneous (dermal or plexiform) benign neurofibromas. Plexiform neurofibromas can give rise to malignant peripheral nerve sheath tumors, which are resistant to conventional therapies.

Experimental Design: To identify new signaling pathways involved in the malignant transformation of plexiform neurofibromas, we applied a 22,000-oligonucleotide microarray approach to a series of plexiform neurofibromas and malignant peripheral nerve sheath tumors. Changes in the expression of selected genes were then confirmed by real-time quantitative reverse transcription-PCR.

Results: We identified two *tenascin* gene family members that were significantly deregulated in both human NF1-associated tumors and *NF1*-deficient primary cells: *Tenascin C* (*TNC*) was up-regulated whereas *tenascin XB* (*TNXB*) was down-regulated during tumor progression. TNC activation is mainly due to the up-regulation of large *TNC* splice variants. Immunohistochemical studies showed that *TNC* transcripts are translated into TNC protein in *TNC*-overexpressing tumors. Aberrant transcriptional activation of *TNC* seems to be principally mediated by activator protein transcription factor complexes.

Conclusion: *TNXB* and *TNC* may be involved in the malignant transformation of plexiform neurofibromas. Anti-TNC antibodies, already used successfully in clinical trials to treat malignant human gliomas, may be an appropriate new therapeutic strategy for NF1.

Authors' Affiliations: [1]Laboratoire de Génétique Moléculaire-Institut National de la Sante et de la Recherche Medicale U745, Faculté des Sciences Pharmaceutiques et Biologiques, Université Paris V, Paris, France; [2]Centre National de la Recherche Scientifique Unité Mixte de Recherche 8125 Bioinformatics Unit and [3]Functional Genomic Unit, Institut Gustave-Roussy, Villejuif, France; [4]Département d'Anatomo-Cytopathologie and [5]Département d'Dermatologie, AP-HP and Université Paris XII, Hôpital Henri-Mondor, Créteil, France; [6]Laboratoire de Pathologie, Erasmus University Hospital, Université Libre de Bruxelles, Brussels, Belgium; and [7]Laboratoire d'Oncogénétique, Institut National de la Sante et de la Recherche Medicale U735, Centre René Huguenin, St-Cloud, France

Received 1/25/06; revised 9/19/06; accepted 9/27/06.

Grant support: Association pour la Recherche sur le Cancer, Association Neurofibromatoses et Recklinghausen, and Ministère de l'Enseignement Supérieur et de la Recherche.

The costs of publication of this article were defrayed in part by the payment of page charges. This article must therefore be hereby marked *advertisement* in accordance with 18 U.S.C. Section 1734 solely to indicate this fact.

Note: Supplementary data for this article are available at Clinical Cancer Research Online (http://clincancerres.aacrjournals.org/).

Requests for reprints: Ivan Bièche, Laboratoire de Génétique Moléculaire-Institut National de la Sante et de la Recherche Medicale U745, Faculté des Sciences Pharmaceutiques et Biologiques, Université Paris 5, 4 avenue de l'Observatoire, 75006 Paris, France. Phone: 33-1-53-73-97-25; Fax: 33-1-44-07-17-54; E-mail: ivan.bieche@univ-paris5.fr.

doi:10.1158/1078-0432.CCR-06-0182

Neurofibromatosis type 1 (NF1) is an autosomal dominant neurocutaneous disorder that affects 1 in 3,000 individuals worldwide (1). The *NF1* gene, located on chromosome 17q11.2, was identified by positional cloning, and its protein product, neurofibromin, functions as a tumor suppressor (2, 3). Neurofibromin contains a central domain homologous to the Ras-GTPase–activating protein family, which functions as negative regulators of Ras proteins (4).

The main clinical features of NF1 are *café au lait* macules, skinfold freckling, and iris Lisch nodules. Patients are at an increased risk of both benign and malignant tumors, and NF1 is thus classified as a tumor predisposition syndrome. The most common tumors are benign peripheral nerve sheath tumors (neurofibromas), which vary greatly in both number and size, and may be dermal or plexiform (5). In contrast to dermal neurofibromas, which are typically small and which grow as discrete lesions in the dermis, plexiform neurofibromas can develop internally along the plexus of major peripheral nerves and become quite large (6). Both dermal and plexiform neurofibromas are heterogeneous tumors mainly composed of Schwann cells (60-80%), together with fibroblasts, mast cells, and other cells.

In about 5% of patients with NF1, neurofibromas (mainly plexiform neurofibromas) progress to malignant peripheral nerve sheath tumors (MPNST). More than 80% of MPNSTs are high-grade malignant tumors, corresponding to WHO grades 3 and 4 (7). MPNSTs are resistant to conventional therapies, and their deep-seated position and locally invasive growth hinder complete surgical resection. The 5-year survival rate among patients with MPNSTs ranges from 30% to 50%. Schwann cells are considered to be the progenitors of both neurofibromas and MPNSTs, but recent data suggest that other cell types may contribute to the development of these tumors (8).

The molecular mechanisms responsible for malignant progression of neurofibromas are largely unknown. Only a few relevant genetic alterations have thus far been identified (9, 10). In keeping with its role as a classic tumor-suppressor gene, *NF1* loss of heterozygosity has been found in NF1-associated MPNSTs, but also in benign neurofibromas (11). *TP53* mutations have been identified in MPNSTs but not in benign neurofibromas, indicating that the p53-mediated pathway is involved in tumor progression (12–14). Consistent with a role of p53 in the progression of MPNSTs, mice that harbor both *NF1* and *TP53* mutations develop MPNSTs (15). Alterations of other genes (*p16/CDKN2A*, *p14/ARF*, *p27/KIP1*, *EGFR*, and *mTOR*) are frequent in MPNSTs but not in neurofibromas (16–21). Together, these findings suggest that the loss of *NF1* initiates tumor formation and that malignant progression requires additional genetic lesions.

The recent development of efficient tools for large-scale analysis of gene expression has provided new insights into the involvement of gene networks and regulatory pathways in various tumoral processes (22). These methods include microarrays, which can be used to analyze the expression of thousands of genes at a time, and real-time reverse transcription-PCR (RT-PCR) assays for more accurate and quantitative expression analysis of smaller numbers of candidate genes (23).

Using large-scale, real-time RT-PCR, we have previously characterized a set of 30 genes discriminating between dermal and plexiform neurofibromas (23), as well as an independent set of 28 genes involved in the malignant transformation of plexiform neurofibromas into MPNSTs (24). We also identified a five-gene signature (*MMP9*, *VEGFR3*, *TRAILR2*, *SHH*, and *GLI1*) that predicted the clinical course of plexiform neurofibromas (23).

Here, we did a genomewide microarray analysis of six plexiform neurofibroma samples and four MPNST samples. We identified 74 genes whose expression differed between the two sample types, including two members of the *tenascin* gene family, *tenascin C* (*TNC*) and *tenascin XB* (*TNXB*). Changes in the expression of these *tenascin* genes were then confirmed by real-time quantitative RT-PCR in a larger series of dermal and plexiform neurofibromas and MPNSTs, as well as human *NF1*-deficient primary cells. We also investigated the involvement of large *TNC* splice variants in NF1 tumorigenesis.

Materials and Methods

Patients and samples

Samples of 14 plexiform neurofibromas and 10 MPNSTs were obtained by surgical excision from patients with NF1 at Henri Mondor Hospital (Creteil, France).

The main clinical and histologic characteristics of the 10 patients with MPNSTs are shown in Supplementary Table S1. The MPNSTs all arose from plexiform neurofibromas and showed very weak S100 immunostaining.

Twenty dermal neurofibromas were used as "normal" control samples because they are not at risk of developing into malignant MPNSTs. Neurofibromas are heterogeneous benign tumors composed of Schwann cells, fibroblasts, mast cells, and other cells, and have no "normal" tissue equivalent. Gene expression levels in plexiform neurofibromas and MPNSTs, determined by oligonucleotide microarray and real-time RT-PCR analyses, were thus expressed relative to the expression levels in dermal neurofibromas (obtained by laser excision).

Immediately after surgery, the tumor samples were flash frozen in liquid nitrogen and stored at −80°C until RNA extraction.

Primary cell culture and differential isolation of Schwann cells and fibroblasts from neurofibromas

Cell culture conditions were mainly realized as described by Bachelin et al. (25). Briefly, the neurofibromas were cut into fragments, and explants were seeded in 25-cm^2 flasks coated with collagen type I (2 μg/mL; Sigma, St. Louis, MO) and fed with Schwann cell medium composed of 10% DMEM-fetal bovine serum, 100 μg/mL penicillin, 100 units/mL streptomycin, 1 μg/mL forskolin (Sigma), 10 μg/mL insulin (Sigma), and 10 ng/mL heregulin $\beta1_{176-246}$ (R&D Systems, Minneapolis, MN). A combination of differential adhesion behavior during trypsinization and forskolin treatment was used to separate fibroblasts from Schwann cells after three to four passages of neurofibroma explants. Cells were fed with 10% DMEM-fetal bovine serum, 100 μg/mL penicillin, and 100 units/mL streptomycin (fibroblasts) or with Schwann cell medium, and were incubated at 37°C in humidified air containing 7.5% or 5% CO_2 (Schwann cells and fibroblasts, respectively). The percentage of contaminating fibroblasts or Schwann cells in each culture was determined by immunostaining using rabbit polyclonal antibody directed against the human S100A and S100B proteins (DAKO, Glostrup, Denmark) as described by Rosenbaum et al. (26).

Oligonucleotide microarrays

We used oligonucleotide microarrays to analyze six plexiform neurofibromas and four MPNSTs. A pool composed of equal amounts of total RNA from two dermal neurofibromas was used as the RNA reference. The quality of the 12 tumor total RNAs, based on the 28S/18S rRNA ratio, was assessed by using the RNA 6000 Nano Lab-On-chip, developed on the Agilent 2100 Bioanalyzer device (Agilent Technologies, Palo Alto, CA). Five hundred nanograms of total RNA from each tumor sample and from the RNA reference pool were used to generate labeled antisense cRNAs with T7 RNA polymerase.

We used the Agilent 22K Human 1A (G4110A) long (60-bp) oligonucleotide microarray and the dual-color analysis method in which probes from tumor samples and from reference RNA are differentially labeled with cyanine 5 and cyanine 3. These microarrays, developed by Agilent Technologies, have 22,000 features, representing 16,840 known unique human genes. Labeling of cRNA was done with cyanine 5–CTP for all samples and cyanine 3–CTP for the RNA reference pool. Reverse transcription, linear amplification, cRNA labeling, and purification were done using the Agilent Linear Amplification kit. Hybridization was run for 17 h at 60°C, with 1 μg of cyanine 5–labeled cRNA from each tumor mixed with the same amount of cyanine 3–labeled cRNA from the reference pool. The arrays were then washed with 0.6× and 0.01× SSC buffers containing Triton and dried with a nitrogen gun. Microarrays were scanned with the Agilent DNA Microarray Scanner. The fluorescence images were quantified using the Feature Extraction software (Agilent Technologies).

All data obtained by microarray analysis have been submitted to ArrayExpress at the European Bioinformatics Institute[8] with the accession number E-TABM-69. ArrayExpress is a public repository for

[8] http://www.ebi.ac.uk/arrayexpress/.

microarray data, aimed at storing well-annotated data in accordance with Microarray Gene Expression Data recommendations.[9]

Microarray data analysis was done in part with Rosetta Resolver system for gene expression analysis (Rosetta Inpharmatics LLC, Seattle, WA). All data were filtered to eliminate low-intensity values, the threshold (under 200 arbitrary units for both colors) being based on the linearity test. Each selected gene had at least a 2-fold change, with a P value of spot in the microarray image <0.001, indicating a high differential expression of the patient's sample compared with the reference pool. Using this procedure, 6,773 genes passed the filter. For unsupervised clustering, we used a hierarchical agglomerative algorithm that pair samples according to a Pearson-based distance. ANOVA was applied to the microarray data to discriminate between plexiform neurofibromas and MPNSTs.

Real-time RT-PCR

Tenascin gene mRNA quantification. The theoretical and practical aspects of real-time quantitative RT-PCR using the ABI Prism 7700 Sequence Detection System (Perkin-Elmer Applied Biosystems, Foster City, CA) have been described in detail elsewhere (27).

The precise amount of total RNA added to each reaction mix (based on absorbance) and its quality (i.e., lack of extensive degradation) are both difficult to assess. We therefore also quantified transcripts of two endogenous RNA control genes involved in two cellular metabolic pathways, namely, *TBP* (Genbank accession no. NM_003194), which encodes the TATA box-binding protein (a component of the DNA-binding protein complex transcription factor II D), and *RPLP0* (also known as 36B4; Genbank accession no. NM_001002), which encodes the human acidic ribosomal phosphoprotein P0. *TBP* and *RPLP0* were selected as endogenous controls because the levels of their transcripts in the tumor samples are low (C_t values between 24 and 26) and high (C_t values between 18 and 20), respectively.

Each sample was normalized on the basis of its *TBP* (or *RPLP0*) content.

Results, expressed as N-fold differences in target gene expression relative to the *TBP* (or *RPLP0*) gene and termed N_{target}, were determined as $N_{target} = 2^{\Delta Ct\ sample}$, where the ΔC_t value of the sample was determined by subtracting the average C_t value of the target gene from the average C_t value of the *TBP* (or *RPLP0*) gene (27, 28).

The nucleotide sequences of the oligonucleotide primers used to amplify *TBP*, *RPLP0*, and the *tenascin* genes are shown in Supplementary Table S2. To avoid amplification of contaminating genomic DNA, one of the two primers was placed at the junction between two exons.

The RNA extraction, cDNA synthesis, and PCR reaction conditions are described elsewhere (27).

Proportion of TNC splice variants. TNC exists in multiple variants, owing to alternative spliced exons coding fibronectin type III (FNIII) domains. Fully truncated TNC (TNC-ft) contains eight FNIII domains (Supplementary Fig. S1). Larger variants of the molecule are generated by alternative splicing of additional FNIII modules between the fifth and sixth FNIII domains of the basic structure. Nine alternatively spliced FNIII domains have been identified for human TNC. Because these alternatively spliced modules are encoded by single exons, the variable domains might be spliced independently of each other, giving rise to a multitude of different variants (512 in theory). Some studies have identified at least 22 different human *TNC* splice variants (29). Thus, to quantify *TNC* splice variants, we used the following real-time RT-PCR approach: TNC-ft was specifically amplified by using one of the two primers (upper primer) placed at the junction between the exon coding for FNIII domain 5 and the exon coding for FNIII domain 6. The *TNC* splice variants were amplified by using the two primers both placed on the same exons. The positions of the primers on the *TNC* gene are shown in Supplementary Fig. S1, and their nucleotide sequences are shown in Supplementary Table S2.

[9] http://www.mged.org.

For a given sample, the result was expressed as a proportion (P_v, a percentage) of the *TNC-ft* mRNA level over the sum of the mRNA level of the *TNC-ft* and the mRNA level of the most strongly expressed spliced exon (*TNC-v*) among the nine putative additional *TNC* exons. The following formula was used:

$$P_v = 100 \times \frac{TNC\text{-}ft \text{ mRNA level}}{TNC\text{-}ft \text{ mRNA level} + TNC\text{-}v \text{ mRNA level}}$$

Statistical analysis. Because the mRNA levels did not fit a Gaussian distribution, (*a*) the mRNA levels in each subgroup of samples were expressed as their median values and ranges, rather than their mean values and coefficients of variation; and (*b*) relationships between the molecular markers and clinical and biological variables were tested by using the nonparametric Mann-Whitney U test (30). Differences between two populations were judged significant at confidence levels >95% ($P < 0.05$).

To visualize the capacity of a given molecular marker to discriminate between two populations (in the absence of an arbitrary cutoff value), we summarized the data in a receiver operating characteristic curve (31). The area under the curve was calculated as a single index of the discriminatory capacity of each candidate molecular marker. When a molecular marker had no discriminatory value, the receiver operating characteristic curve lies close to the diagonal, and the area under the curve is close to 0.5. When a marker has a strong discriminatory value, the receiver operating characteristic curve moves to the upper left-hand corner (or the lower right-hand corner), and the area under the curve is close to 1.0 (or 0).

Immunohistochemical studies

Indirect immunoperoxidase staining of fixed tissues was done using mouse monoclonal antibody clone DB7 directed against the human TNC protein (Chemicon International, Temecula, CA) at a 1:200 dilution.

Five-micrometer-thick sections were submitted to standard immunohistochemistry, as previously detailed (32). Immunohistochemical expression was visualized by means of streptavidin-biotin-peroxidase complex kit reagents (BioGenex, San Ramon, CA) with diaminobenzidine/H_2O_2 as the chromogenic substrate (32). Negative control sections were immunostained under the same conditions, but using nonimmune serum (DAKO) as primary antibody.

The localization and intensity of staining were assessed by two independent pathologists who were blinded to the real-time RT-PCR results.

Results

Screening for differentially expressed genes. Microarray experiments based on dual-color technology were done on 10 NF1-associated tumors (six plexiform neurofibroma and four MPNSTs) by comparison to a RNA reference pool (prepared by mixing identical amounts of RNA from two dermal neurofibromas).

Using the Resolver software, an intensity and fold change–based filtering approach (>2-fold change and $P < 0.001$) selected 6,773 features from among the 22,000 present on the 60-mer oligonucleotide microarray. Unsupervised hierarchical clustering of these 6,773 features (Fig. 1) showed that the tumor samples fell into four subgroups, one of which contained all four MPNSTs. The other three subgroups each contained two plexiform neurofibromas. Interestingly, two of the six plexiform neurofibromas subsequently developed into MPNSTs, and both segregated together, forming one of the four subgroups.

ANOVA showed that 74 genes were differentially expressed ($P < 10^{-7}$) between plexiform neurofibromas and MPNSTs; 46

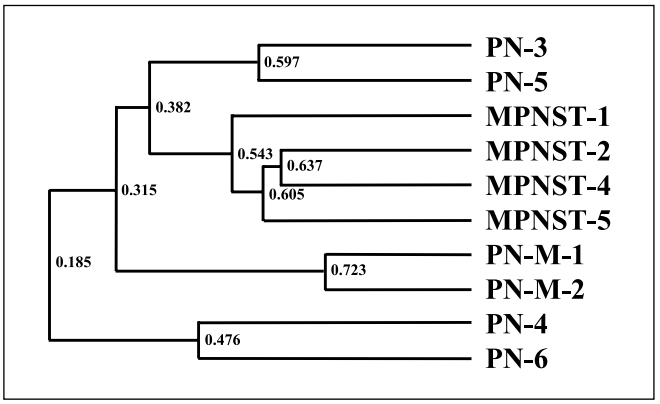

Fig. 1. Unsupervised hierarchical clustering of four MPNSTs and six plexiform neurofibromas [four plexiform neurofibromas not associated with MPNST (*PN*) and two plexiform neurofibromas associated with MPNST (*PN-M*)]. The classification is based on the 6,773 filtered microarray features using an agglomerative algorithm based on the Pearson's correlation coefficient.

genes were up-regulated, and 28 were down-regulated in MPNSTs (Supplementary Table S3).

Supervised hierarchical clustering, based on the expression of the 74 differentially expressed genes, perfectly discriminated between the four plexiform neurofibromas not associated with MPNST, the two plexiform neurofibromas associated with MPNST, and the four MPNSTs (Supplementary Fig. S2).

The up-regulated genes of known function were mainly involved in cell proliferation (*CCNB2*, *CCND2*, *CDK4*, *DNMT3A*, and *TOP2A*), cell cycle control (*ANAPC11*, *PKMYT1*, *PRC1*), and apoptosis (*BIRC5/Survivin*). Several of the down-regulated genes were Schwann cell specific (*ITGB4*) or mast cell specific (*TPSB*), pointing to a depletion and/or dedifferentiation of Schwann cells and mast cells during the malignant transformation of plexiform neurofibromas.

Expression changes of several genes identified by oligonucleotide microarray screening, i.e., four up-regulated genes (*BIRC5/Survivin*, *SPP1*, *TOP2A*, and *OSF-2*) and two down-regulated genes (*ITGB4* and *TPSB*), were confirmed by real-time quantitative RT-PCR in a series of dermal neurofibromas, plexiform neurofibromas, and MPNSTs (Supplementary Table S4).

Together, these results are in keeping with our previous molecular profiling results for NF1-associated MPNSTs, based on large-scale, real-time RT-PCR (24), and with data from recent gene expression profiling studies of NF1-associated tumors (33, 34).

We further explored the four members of the tenascin family (*TNC*, *TNXB*, *TNN*, and *TNR*) because two (*TNC* and *TNXB*) were among the 74 genes differentially expressed between plexiform neurofibromas and MPNSTs (*TNN* was not included in the 22,000-feature oligonucleotide microarray). *TNC* was up-regulated, whereas *TNXB* was down-regulated, suggesting that the two genes have opposite functions.

mRNA expression of* TNC, TNXB, TNN, *and* TNR *in 20 dermal neurofibromas, 14 plexiform neurofibromas, and 10 MPNSTs. *TNR* mRNA were detectable but not reliably quantifiable by means of real-time quantitative RT-PCR assay ($C_t > 35$) in the MPNSTs and plexiform and dermal neurofibromas. The mRNAs of the three other genes were reliably quantifiable in the three types of sample: *TNN* expression was moderate ($26 < C_t < 28$), whereas *TNC* and *TNXB* expression was strong ($C_t < 24$).

Table 1 shows the median values (and range) of *TNC*, *TNXB*, and *TNN* mRNA levels in the three groups of tumor samples. For each gene, mRNA levels were normalized such that the median value of the 20 dermal neurofibromas was 1. *TNC* was significantly up-regulated in both the plexiform neurofibromas (~3-fold) and the MPNSTs (~5-fold) compared with the dermal neurofibromas ($P = 0.003$; Table 1). It is noteworthy that 4 of the 14 patients with plexiform neurofibromas developed MPNST. The mRNA levels of *TNC* showed a trend toward significance ($P = 0.11$) between the four plexiform neurofibromas associated with MPNST (R_{TNC} values from 2.92 to 8.31; median, 4.98) and the 10 plexiform neurofibromas not associated with MPNST (R_{TNC} values from 0.26 to 8.20; median, 1.87).

TNXB was significantly down-regulated in MPNSTs alone (>20-fold; $P = 0.0003$; Table 1). Finally, *TNN* was not significantly altered in either the plexiform neurofibromas or the MPNSTs, despite slight (nonsignificant) down-regulation (~2-fold).

The mRNA levels shown in Table 1 (calculated as described in Materials and Methods) show the abundance of the *tenascin* genes relative to the endogenous control (*TBP*) used to normalize the starting amount and quality of total RNA. Similar results were obtained with a second endogenous control, *RPLP0* (also known as 36B4).

mRNA expression of* TNC, TNXB, *and* TNN *in normal human cells. Both neurofibromas and MPNSTs are heterogeneous tumors mainly composed of Schwann cells (60-80%), together with fibroblasts, mast cells, endothelial cells, and other cells.

To further investigate the cell type specificity of *TNC*, *TNXB*, and *TNN* expression, we analyzed the mRNA levels of these three genes by means of real-time RT-PCR in normal mast cells, Schwann cells, fibroblasts, and endothelial cells (Fig. 2).

Table 1. mRNA levels of *TNC*, *TNXB*, and *TNN* in dermal neurofibromas, plexiform neurofibromas, and MPNSTs

Genes	Gene aliases	Gene definition	Dermal neurofibromas ($n = 20$)	Plexiform neurofibromas ($n = 14$)	MPNSTs ($n = 10$)	P^*
TNC	HXB	Tenascin C (hexabrachion)	1.00 (0.25-4.43)†	2.98 (0.26-8.31)	4.95 (1.81-18.45)	0.0003
TNXB	TNX	Tenascin XB	1.00 (0.12-3.09)	1.75 (0.12-5.48)	0.03 (0.00-0.39)	0.00003
TNN	TNN	Tenascin N	1.00 (0.18-6.70)	0.32 (0.01-5.92)	0.44 (0.01-4.91)	NS

Abbreviation: NS, not significant.
*Mann-Whitney *U* test: dermal neurofibromas versus plexiform neurofibromas versus MPNSTs.
†Median (range) of gene mRNA levels.

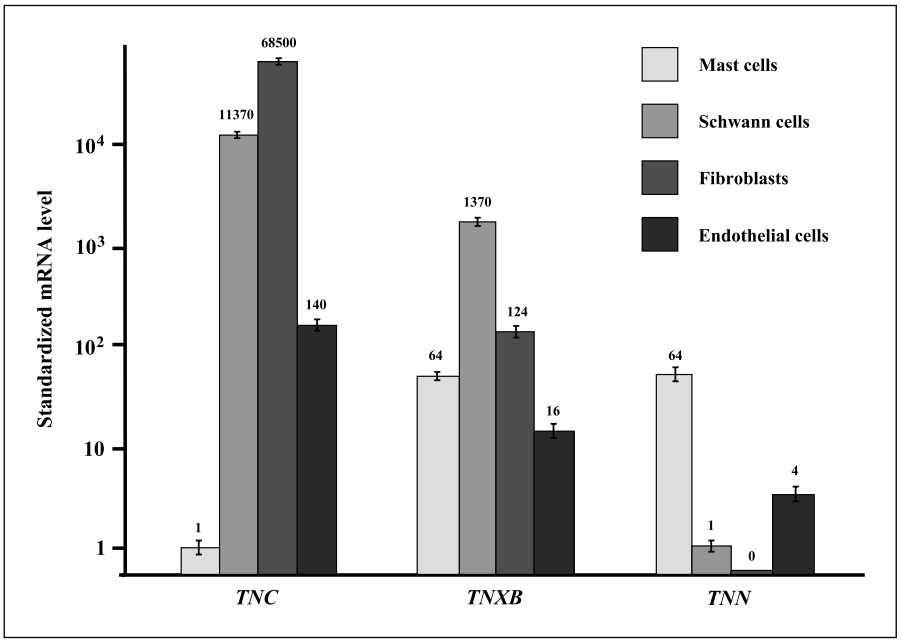

Fig. 2. mRNA expression of *TNC*, *TNXB*, and *TNN* in normal human mast cells, Schwann cells, fibroblasts, and endothelial cells. For each gene, mRNA levels were normalized such that the value for the "basal mRNA level" (smallest amount of target gene mRNA quantifiable, $C_t = 35$) was 1. Columns, means of mRNA levels from at least three independent experiments; bars, SD.

TNC was mainly expressed in Schwann cells and fibroblasts and very weakly (100-fold lower) in endothelial cells. *TNXB* was mainly expressed in Schwann cells (10 times more strongly than in the other three cell types). *TNN* expression was moderate in mast cells and weak in the other cell types.

mRNA expression of* TNC *and* TNXB *in neurofibroma-derived primary Schwann cells and primary fibroblasts. *TNC*, which is mainly expressed in Schwann cells and fibroblasts (Fig. 2), was moderately up-regulated in both *NF1*-deficient primary Schwann cells (1.65-fold) and *NF1*-deficient primary fibroblasts (1.65-fold; Fig. 3).

TNXB, which is mainly expressed in normal Schwann cells (Fig. 2), was strongly down-regulated in *NF1*-deficient Schwann cells (decrease >50-fold; Fig. 3).

Proportion of* TNC *splice variants in 20 dermal neurofibromas, 14 plexiform neurofibromas, and 10 MPNSTs. Figure 4 shows the median and range of total *TNC* mRNA levels and the percentage of *TNC* splice variants (determined as indicated in Materials and Methods) in the three groups of tumor samples. Total *TNC* mRNA levels were normalized such that the median value for the 20 dermal neurofibromas was 1.

The proportion of *TNC* splice variants was significantly increased in both MPNSTs (median, 60.3%; range, 13.7-97.8%)

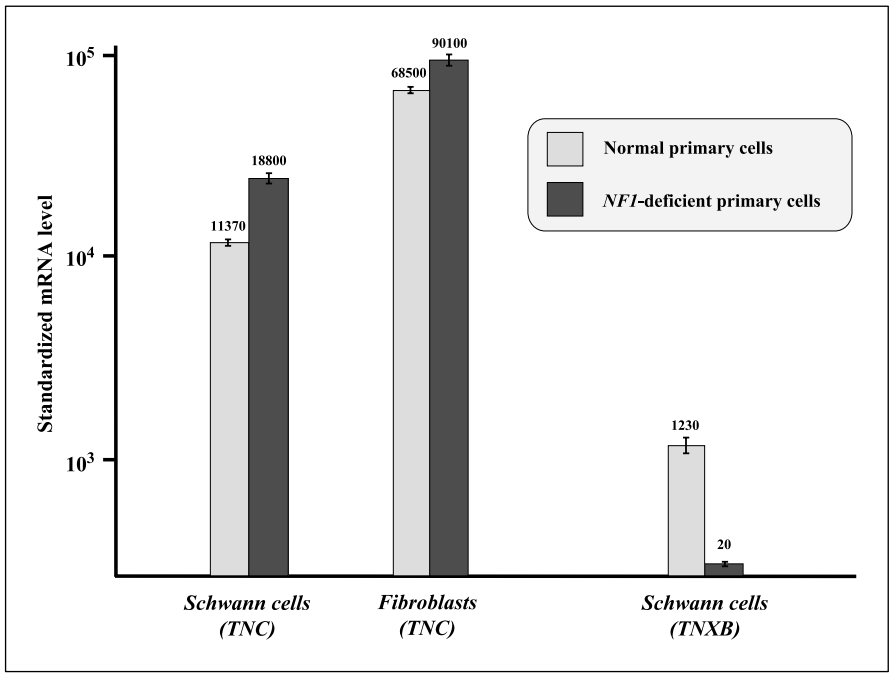

Fig. 3. mRNA expression of *TNC* and *TNXB* in normal and *NF1*-deficient primary Schwann cells and primary fibroblasts. For each gene, mRNA levels were normalized such that the value for the "basal mRNA level" was 1. Columns, mean mRNA levels from at least three independent experiments; bars, SD.

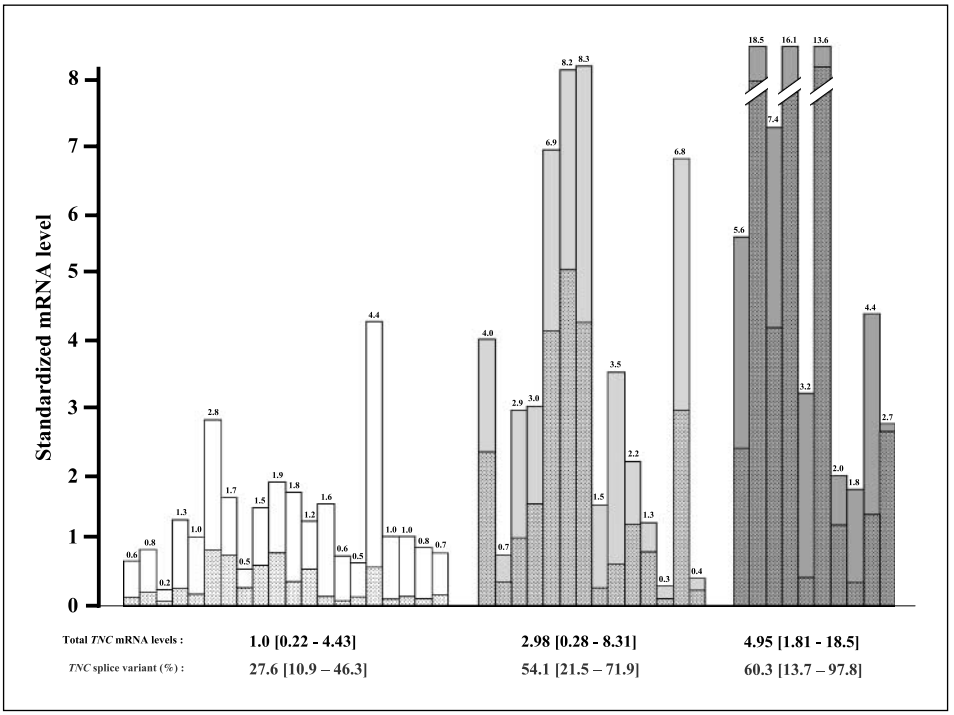

Fig. 4. mRNA levels of total *TNC* and proportion of *TNC* splice variants in 20 individual dermal neurofibromas (*white columns*), 14 plexiform neurofibromas (*light-gray columns*), and 10 MPNSTs (*dark-gray columns*). Median values (and ranges) are indicated for each tumor subgroup.

and plexiform neurofibromas (median, 54.1; range, 21.5-71.9%) compared with dermal neurofibromas (median, 27.6%; range, 10.9-46.3%; $P = 0.0007$).

It is noteworthy that the highest proportion of *TNC* splice variants ($P_v > 90\%$) was observed exclusively in the MPNST samples (3 of 10 MPNSTs).

The analysis of the four cases in which both a plexiform neurofibroma and a matched MPNST were investigated showed a clear association between the increase in the total *TNC* mRNA level and the increase of the proportion of *TNC* splice variants, during progression from plexiform neurofibroma to MPNST, as in patients 1 and 2 (Fig. 5).

Immunohistochemical studies. Of the 12 tumors (three dermal neurofibromas, four plexiform neurofibromas, and five MPNSTs) studied by immunohistochemistry, specific TNC immunoreactivity was detected in the five tumors that overexpressed *TNC* mRNA (two plexiform neurofibromas and three MPNSTs), but in none of the seven tumors showing normal *TNC* expression (three dermal neurofibromas, two plexiform neurofibromas, and two MPNSTs). We thus observed a perfect

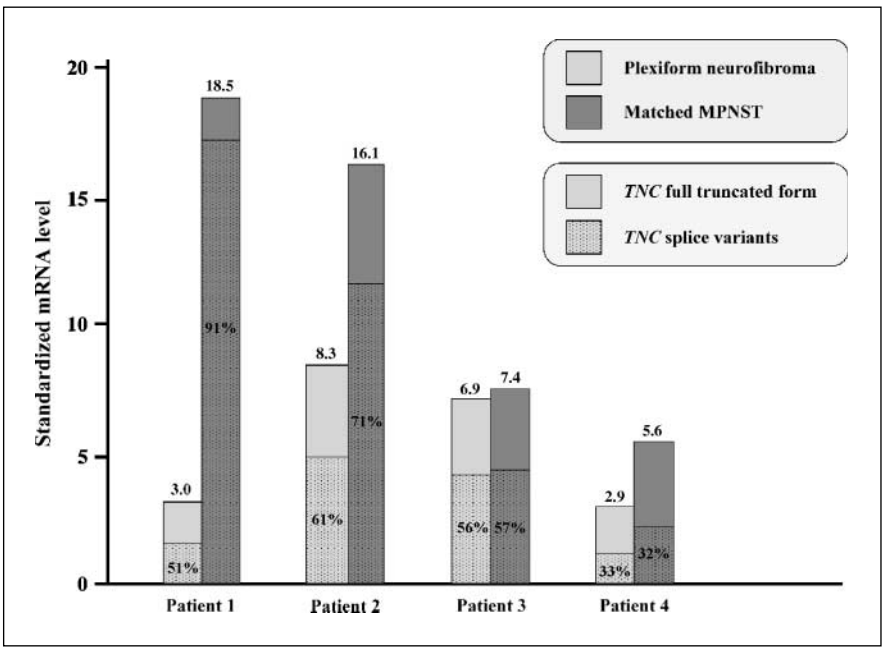

Fig. 5. mRNA levels of total *TNC* and the proportion of *TNC* splice variants in four tumor pairs (plexiform neurofibroma and matched MPNSTs from the same patient). mRNA levels of total *TNC* and the proportion of *TNC* splice variants are indicated for each tumor sample.

match between *TNC* mRNA overexpression and TNC immunoreactivity in tumor cells.

In tumors normally expressed *TNC* mRNA, TNC immunoreactivity was exclusively found around follicular structures (Fig. 6A) and beneath the epidermis, whereas tumoral stroma and tumor cells were negative.

In plexiform neurofibromas that overexpressed *TNC* mRNA, TNC showed focal and weak positivity in the tumoral stroma, whereas a strong staining was seen in the perineurium (Fig. 6B) and was weak in the tumor cells.

In MPNSTs that overexpressed *TNC* mRNA, TNC showed focal but strong positivity in the tumoral stroma (Fig. 6C). TNC immunoreactivity was observed in the cytoplasm of scattered tumor cells (Fig. 6D).

Relationship between the mRNA levels of* TNC *and various genes possibly involved in* TNC *deregulation in NF1. *In vitro* studies of the *TNC*-responsive promoter elements have suggested that *TNC* gene transcription may be regulated by activator protein-1 (AP-1), nuclear factor-κB (NF-κB), or KROX24/early growth response 1 (KROX24/EGR1; ref. 35). To explore the possible involvement of these three transcriptional complexes in the up-regulation of *TNC* in NF1-associated tumors, we tested the relationship between the expression of 24 candidate genes possibly involved in the AP-1, NF-κB, or KROX24/EGR1 pathways in three normal *TNC*-expressing MPNSTs and three *TNC*-overexpressing MPNSTs. These 24 selected genes encode KROX24/EGR1, the different subunits of AP-1 and NF-κB, and various well-known AP-1– and NF-κB–induced genes. The results of these analyses are summarized in Table 2. We found total positive associations (area under the curve-receiver operating characteristic, 1.000) between *TNC* and six other genes, namely, *JUN*, *JUND*, and *ATF3* (AP-1 subunit genes); *MMP1* (an AP-1–induced gene); *RELB* (NF-κB subunit); and *IER3S* (an NF-κB–induced gene). Supplementary Fig. S3 shows the mRNA levels of the six *TNC*-associated genes in each MPNST sample.

Discussion

To identify a new outstanding signaling pathway involved in malignant transformation of plexiform neurofibromas, we applied an initial screening approach based on a 22,000-feature oligonucleotide microarray to a series of plexiform neurofibromas and MPNSTs. Nonsupervised hierarchical clustering failed to perfectly distinguish between benign and malignant tumoral tissues, probably because of the small number of samples. However, statistical analysis revealed distinct differences between plexiform neurofibromas and MPNSTs. Indeed, we observed a significant difference ($P < 10^{-7}$, ANOVA test) in the expression level of 74 genes between these two tumor populations. Many of these genes encode proteins that are involved in cell proliferation (*CCNB2*, *CCND2*, *CDK4*, *DNMT3A*, and *TOP2A*), cell cycle control (*ANAPC11*, *PKMYT1*, and *PRC1*), and apoptosis (*BIRC5*/*Survivin*). These results are thus not very original because they are in keeping with general concepts of tumorigenesis, in which alterations of these pathways are common. Moreover, several of the down-regulated genes were Schwann cell specific (*ITGB4*) or mast cell specific (*TPSB*), pointing to depletion and/or dedifferentiation of Schwann cells and mast cells during the malignant transformation of plexiform neurofibromas. Together, these results are in keeping with our previous molecular profiling results for NF1-associated MPNSTs based on large-scale real-time RT-PCR (24) and with data from recent gene expression profiling studies of NF1-associated tumors and cell lines (33, 34). For example, Miller et al. (34) identified a

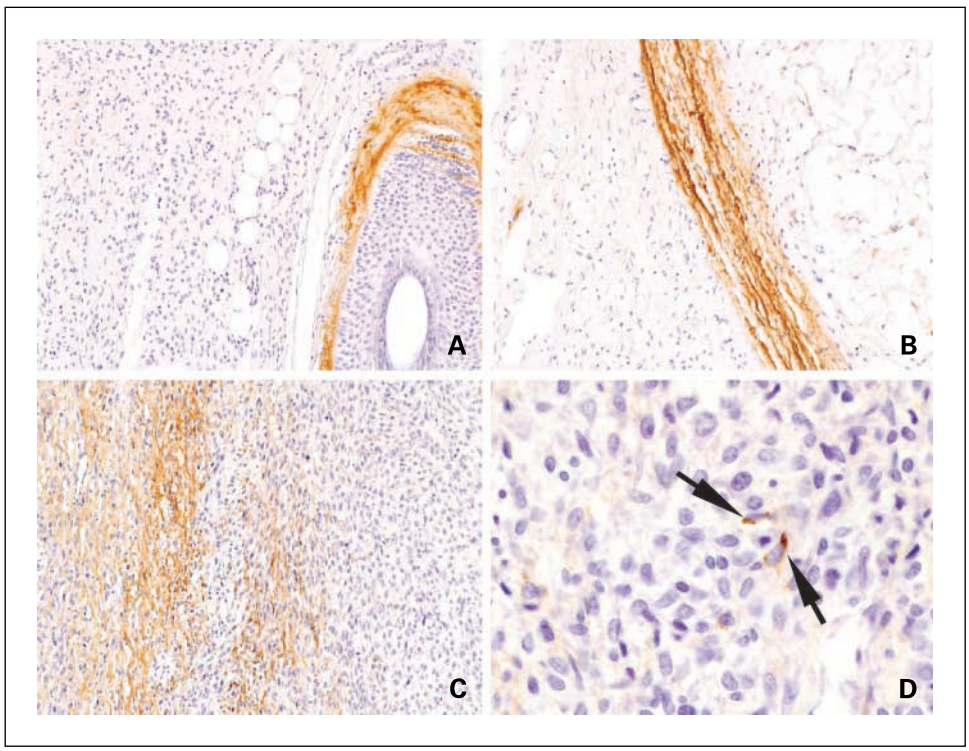

Fig. 6. Immunohistochemistry staining of TNC in NF1-associated tumors. *A,* dermal neurofibroma shows no staining for TNC, whereas immunoreactivity is seen around the basement membrane of the pilar sheath of a normal follicular structure. *B,* strong TNC staining is seen in the perineurium, at the periphery of a nodular structure from a plexiform neurofibroma. *C,* MPNST with focal but strong TNC staining in the extracellular fibrotic matrix. *D,* TNC immunoreactivity is localized in the cytoplasm of scattered tumor cells (*arrows*) in a MPNST.

Table 2. Relationship between mRNA levels of *TNC* and various genes possibly involved in *TNC* deregulation in NF1

Genes	Gene definitions	Normal *TNC*-expressed MPNSTs (*n* = 3)	*TNC*-overexpressed MPNSTs (*n* = 3)	ROC-AUC
TNC	Tenascin C (hexabrachion)	1.80 (1.49-2.28)*	7.45 (7.15-9.70)	1.000
AP-1 subunit genes				
JUN	Jun oncogene	0.59 (0.34-0.81)	2.13 (1.45-3.91)	1.000
JUNB	Jun B oncogene	0.87 (0.11-1.30)	1.51 (0.93-17.5)	0.889
JUND	Jun D oncogene	1.02 (0.98-1.13)	4.01 (2.78-5.30)	1.000
FOS	Fos oncogene	0.11 (0.05-1.21)	0.54 (0.26-0.97)	0.667
FOSB	Fos B oncogene	0.12 (0.04-1.06)	0.40 (0.29-0.52)	0.667
ATF3	Activating transcription factor 3	0.62 (0.35-1.59)	2.57 (1.90-2.97)	1.000
AP-1 – induced genes				
MMP1	Matrix metalloproteinase 1	1.60 (0.40-4.31)	68.1 (11.9-182)	1.000
MAP3K8	Mitogen-activated protein kinase kinase kinase 8	0.43 (0.14-0.77)	1.99 (0.10-5.47)	0.667
NF-κB subunit genes				
NFKB1	Nuclear factor of κ light polypeptide gene (p105)	0.72 (0.39-1.91)	3.98 (1.00-6.29)	0.889
NFKB2	Nuclear factor of κ light polypeptide gene (p49)	1.01 (0.94-3.56)	11.8 (2.18-16.6)	0.889
REL	V-rel reticuloendotheliosis viral oncogene homologue	1.03 (0.79-1.21)	0.96 (0.55-5.27)	0.444
RELA	V-rel reticuloendotheliosis viral oncogene homologue A	0.44 (0.35-1.34)	4.99 (1.21-6.14)	0.889
RELB	V-rel reticuloendotheliosis viral oncogene homologue B	0.36 (0.29-2.15)	5.56 (2.37-31.2)	1.000
NF-κB – induced genes				
BCL2A	BCL2-related protein A1	0.34 (0.28-1.53)	0.98 (0.96-1.41)	0.667
IER3S	Immediate early response 3 (isoform short)	1.10 (0.32-1.25)	4.14 (2.36-9.98)	1.000
GADD45B	GADD45 β	1.29 (0.43-1.95)	5.87 (1.32-14.9)	0.889
CD40LG	CD40 ligand	0.99 (0.05-1.31)	1.74 (0.20-1.91)	0.778
PTGS2	Prostaglandin-endoperoxide synthetase 2 (cyclooxygenase 2)	1.03 (0.38-1.68)	4.14 (0.57-6.86)	0.778
IL8	Interleukin 8	1.40 (0.19-5.06)	1.64 (0.91-191)	0.667
VEGFA	Vascular endothelial growth factor A	3.05 (1.35-6.53)	38.3 (5.5-69.0)	0.889
ICAM1	Intercellular adhesion molecule 1 (CD54),	1.16 (0.72-4.43)	20.1 (3.52-27.2)	0.889
VCAM1	Vascular cell adhesion molecule 1	1.47 (0.91-1.70)	1.36 (0.65-3.91)	0.444
SELE	E-selectin	0.44 (0.24-0.74)	0.38 (0.00-0.60)	0.333
KROX24/EGR1 pathway				
EGR1	Early growth response 1 (KROX-24)	0.61 (0.27-1.39)	1.25 (0.87-2.15)	0.778

Abbreviation: ROC-AUC, receiver operating characteristics-area under the curve analysis.
*Median (range) of gene mRNA levels.

159-gene molecular signature distinguishing MPNST cell lines from normal Schwann cells, and which mainly includes overexpressed cell proliferation – associated genes (i.e., *MKI67*, *BUB1*, *MAD2L1*, etc.) and underexpressed Schwann cell – specific genes (i.e., *S100B*, *SOX10*, *PMP22*, etc.).

As expected, several of the genes identified in our large-scale, real-time RT-PCR study (24) were in the present set of 74 genes (up-regulation of *BIRC5/Survivin*, *SPP1/Osteopontin*, *TOP2A*, *OSF-2/Periostin*, etc., and down-regulation of *ITGA4*, *TPSB*, etc.). Interestingly, the weakly expressed genes previously identified, such as *DHH*, *TERT*, *FOXM1*, *FOXA2/HNF3B*, etc. (24), were not identified by this microarray-based screening approach. These data confirm that real-time quantitative RT-PCR is complementary to microarrays for molecular tumor profiling. In particular, real-time RT-PCR seems to be far more sensitive than microarrays for identifying weakly expressed genes.

Here, we focused on the four members of the tenascin family (*TNC*, *TNXB*, *TNN*, and *TNR*), because (*a*) two members (*TNC* and *TNXB*) were among the 74 genes differentially expressed between plexiform neurofibromas and MPNSTs (*TNN* was not included in the 22,000-feature oligonucleotide microarray); (*b*) *TNC* was up-regulated, whereas *TNXB* was down-regulated, suggesting opposite functions; (*c*) tenascins are not involved in cell proliferation but in cell – extracellular matrix interactions, which are a key determinant in NF1 tumorigenesis, characterized by numerous tumor-stroma interactions (36); (*d*) tenascins have a major role in the nervous system (precursor cell migration), and *TNC* is a prominent constituent of peripheral nerves (37); and (*e*) finally, the role of tenascins has recently been suggested in NF1 tumorigenesis. Indeed, Karube et al. (38) identified six genes (including *TNC*) up-regulated in MPNSTs by means of cDNA microarray analysis (composed of 886 genes).

The four members of the *tenascin* gene family were thus investigated by real-time quantitative RT-PCR in a larger series of dermal and plexiform neurofibromas and MPNSTs. *TNR* was not expressed by MPNSTs or plexiform and dermal

neurofibromas, in agreement with previous reports. Tenascin-R is expressed exclusively in the central nervous system, where it is mainly secreted by oligodendrocytes (39). *TNN* expression was not significantly different between dermal/plexiform neurofibromas and MPNSTs. As we found that *TNN* was mainly expressed by mast cells (Fig. 2), the slight down-regulation (~2-fold, nonsignificant) observed in both plexiform neurofibromas and MPNSTs was probably due to a lower abundance of mast cells in plexiform neurofibromas and MPNSTs relative to dermal neurofibromas.

More interestingly, *TNC* was significantly up-regulated in both plexiform neurofibromas (~3-fold) and MPNSTs (~5-fold), whereas *TNXB* was significantly down-regulated in MPNSTs alone (>20-fold). This suggests that *TNC* dysregulation could be an earlier event than *TNXB* deregulation in NF1 tumorigenesis. Similar opposite changes in the mRNA expression of *TNC* and *TNXB* has previously been described in heritable cutaneous malignant melanoma (40).

By using immunohistochemical analysis, we showed that *TNC* transcripts are translated into TNC protein in NF1-associated tumors. We also showed a strong correlation between *TNC* mRNA overexpression and TNC protein abundance.

Among the four main cellular components of neurofibromas, i.e., Schwann cell fibroblasts, mast cells, and endothelial cells, we found that *TNC* was mainly expressed by normal human Schwann cells and fibroblasts, whereas *TNXB* was specifically expressed by Schwann cells (Fig. 2). Interestingly, the up-regulation of *TNC* and the down-regulation of *TNXB* were also observed in human *NF1*-deficient primary Schwann cells (*TNC* and *TNXB*) and *NF1*-deficient human primary fibroblasts (*TNC*) compared with normal primary Schwann cells and normal primary fibroblast (Fig. 3), confirming *in vitro* our results obtained *ex vivo* with human tumor biopsy specimens. These latter results suggest that neurofibromin deficiency may play an active role in altered *TNC* and *TNXB* expression in NF1-associated tumors.

TNC and *TNXB* encode glycoproteins that contribute to the extracellular matrix structure and influence the physiology of cells in contact with the tenascin-containing environment. In tumors, altered *TNC* and *TNXB* expression may deregulate cell morphology, growth, and migration by activating various intracellular signaling pathways (35, 36).

TNXB encodes TNX, a protein of unknown function that is mainly expressed in the peripheral nervous system and muscle. TNX deficiency in humans is associated with Ehlers-Danlos syndrome, a generalized connective tissue disorder resulting from altered metabolism of fibrillar collagens (41). $TNXB^{-/-}$ mice show progressive skin hyperextensibility due to altered collagen deposition by dermal fibroblasts (42). Very little is known about the relevance of this gene to cancer biology. However, Matsumoto et al. (43) showed that tumor invasion and metastasis are promoted in mice deficient in TNX through the activation of the *MMP2* and *MMP9* genes. It is noteworthy that we have previously identified *MMP9* as a major gene up-regulated during NF1 tumorigenesis (23, 24).

TNC encodes TNC protein, and its expression correlates with angiogenesis and local infiltration of normal tissues by tumor cells of various carcinomas (35). Moreover, expression of larger *TNC* splice variants correlates with increased cell migration, tissue remodeling, and invasive carcinomas, whereas the fully truncated *TNC* transcript is expressed in more quiescent tissues and is associated with the production of a stable extracellular matrix. In agreement with these studies, we observed an increase in total *TNC* mRNA levels and in the proportion of *TNC* splice variants during NF1-associated tumor progression (Figs. 4 and 5). These *TNC* splice variants represent a potential mechanism leading to impaired cell signaling and downstream functions by modulating binding interactions with various receptors and with other extracellular matrix components. On the other hand, an increase in total *TNC* could activate cell proliferation by direct binding and activation of the epidermal growth factor receptor by the epidermal growth factor–like repeats of TNC (44). It is noteworthy that *EGFR* overexpression is a major genetic event in NF1-associated and sporadic MPNSTs (19, 45).

To further explore the molecular mechanisms underlying *TNC* overexpression in plexiform neurofibromas and MPNSTs, we studied the possible relationship between the expression of the *TNC* gene and that of various candidate genes involved in regulating *TNC* expression. Indeed, several transcription factor complexes, such as NF-κB, AP-1, and KROX24/EGR1, have been shown to regulate the expression of *TNC* promoter reporter constructs (reviewed in ref. 35). Coexpression profiles suggest common functional pathways (46). Our results suggest that *TNC* transcription in NF1-associated neurofibromas could be controlled by the AP-1 complex (in particular the subunits c-Jun, JunD, and activating transcription factor 3) and possibly also by the NF-κB complex (in particular the RelB subunit). In the context of NF1 tumorigenesis, it is interesting to note that the epidermal growth factor/RAS/RAF signaling pathway induces transcription preferentially via the activation of activating transcription factor 3/c-Jun and the activating transcription factor 3/JunD heterodimers (47). Finally, we cannot rule out the possibility that *TNC* gene expression could be regulated by additional factors recently identified such as β-catenin (48) or a functional binding element involving several transcription growth factor-β signaling targets, such as Smad3, Sp1, Ets1, and CBP/p300 (49).

The finding that *TNC* deregulation may participate in NF1-associated tumorigenesis may represent a therapeutic breakthrough in this disease. NF1-associated MPNSTs are devastating, and there is currently no effective treatment. Moreover, plexiform neurofibroma, although benign, can be painful and debilitating and can grow large enough to encompass an entire body region. Many plexiform neurofibromas cannot be surgically resected because of underlying nerve involvement. Radiolabeled anti-TNC antibodies have been used successfully in clinical trials to treat malignant human gliomas (50) and non–Hodgkin's lymphoma (51). However, it is important to note that *TNC*, although abundantly present in tumor cells, is also expressed in some normal cells and tissues (Fig. 6A; ref. 36) and that may pose the problem of the specificity of such therapeutic approach with its potential adverse side effects.

In conclusion, we report the involvement of *TNC* and *TNX* in the genesis of NF1-associated MPNST. Full confirmation of the role of these two genes in NF1 needs further *in vitro* (gain- or loss-of-function experiments in cultured cells) and *in vivo* (animal model) studies. Our results suggest that anti-TNC antibodies, already used with success in other cancers, may represent a new therapeutic strategy for NF1.

References

1. Friedman JM. Epidemiology of neurofibromatosis type 1. Am J Med Genet 1999;89:1–6.
2. Cawthon RM, Weiss R, Xu GF, et al. A major segment of the neurofibromatosis type 1 gene: cDNA sequence, genomic structure, and point mutations. Cell 1990;62:193–201.
3. Wallace MR, Marchuk DA, Andersen LB, et al. Type 1 neurofibromatosis gene: identification of a large transcript disrupted in three NF1 patients. Science 1990; 249:181–6.
4. DeClue JE, Papageorge AG, Fletcher JA, et al. Abnormal regulation of mammalian p21ras contributes to malignant tumor growth in von Recklinghausen (type 1) neurofibromatosis. Cell 1992;69:265–73.
5. Ferner RE, Gutmann DH. International consensus statement on malignant peripheral nerve sheath tumors in neurofibromatosis. Cancer Res 2002;62: 1573–7.
6. Scheithauer B, Woodruff J, Erlandson R. Tumors of the peripheral nervous system. Atlas of tumor pathology. Third series, fascicle 24. Washington, DC: Armed Forces Institute of Pathology; 1999.
7. Woodruff JM. Pathology of tumors of the peripheral nerve sheath in type 1 neurofibromatosis. Am J Med Genet 1999;89:23–30.
8. Zhu Y, Ghosh P, Charnay P, Burns DK, Parada LF. Neurofibromas in NF1: Schwann cell origin and role of tumor environment. Science 2002;296:920–2.
9. Cichowski K, Jacks T. NF1 tumor suppressor gene function: narrowing the GAP. Cell 2001;104: 593–604.
10. Rubin J, Gutmann D. Neurofibromatosis type 1—a model for nervous system tumour formation? Nat Rev Cancer 2005;5:557–64.
11. Legius E, Marchuk DA, Collins FS, Glover TW. Somatic deletion of the neurofibromatosis type 1 gene in a neurofibrosarcoma supports a tumour suppressor gene hypothesis. Nat Genet 1993;3:122–6.
12. Legius E, Dierick H, Wu R, et al. TP53 mutations are frequent in malignant NF1 tumors. Genes Chromosomes Cancer 1994;10:250–5.
13. Leroy K, Dumas V, Martin-Garcia N, et al. Malignant peripheral nerve sheath tumors associated with neurofibromatosis type 1: a clinicopathologic and molecular study of 17 patients. Arch Dermatol 2001;137: 908–13.
14. Menon AG, Anderson KM, Riccardi VM, et al. Chromosome 17p deletions and p53 gene mutations associated with the formation of malignant neurofibrosarcomas in von Recklinghausen neurofibromatosis. Proc Natl Acad Sci U S A 1990;87:5435–9.
15. Cichowski K, Shih TS, Schmitt E, et al. Mouse models of tumor development in neurofibromatosis type 1. Science 1999;286:2172–6.
16. Kourea HP, Orlow I, Scheithauer BW, Cordon-Cardo C, Woodruff JM. Deletions of the INK4A gene occur in malignant peripheral nerve sheath tumors but not in neurofibromas. Am J Pathol 1999;155: 1855–60.
17. Kourea HP, Cordon-Cardo C, Dudas M, Leung D, Woodruff JM. Expression of p27(kip) and other cell cycle regulators in malignant peripheral nerve sheath tumors and neurofibromas: the emerging role of p27(kip) in malignant transformation of neurofibromas. Am J Pathol 1999;155:1885–91.
18. Nielsen GP, Stemmer-Rachamimov AO, Ino Y, Moller MB, Rosenberg AE, Louis DN. Malignant transformation of neurofibromas in neurofibromatosis 1 is associated with CDKN2A/p16 inactivation. Am J Pathol 1999;155:1879–84.
19. DeClue JE, Heffelfinger S, Benvenuto G, et al. Epidermal growth factor receptor expression in neurofibromatosis type 1-related tumors and NF1 animal models. J Clin Invest 2000;105:1233–41.
20. Perrone F, Tabano S, Colombo F, et al. p15INK4b, p14ARF, and p16INK4a inactivation in sporadic and neurofibromatosis type 1-related malignant peripheral nerve sheath tumors. Clin Cancer Res 2003;9: 4132–8.
21. Johannessen CM, Reczek EE, James MF, Brems H, Legius E, Cichowski K. The NF1 tumor suppressor critically regulates TSC2 and mTOR. Proc Natl Acad Sci U S A 2005;102:8573–8.
22. DeRisi J, Penland L, Brown PO, et al. Use of a cDNA microarray to analyse gene expression patterns in human cancer. Nat Genet 1996;14:457–60.
23. Levy P, Bieche I, Leroy K, et al. Molecular profiles of neurofibromatosis type 1-associated plexiform neurofibromas: identification of a gene expression signature of poor prognosis. Clin Cancer Res 2004; 10:3763–71.
24. Levy P, Vidaud D, Leroy K, et al. Molecular profiling of malignant peripheral nerve sheath tumors associated with neurofibromatosis type 1, based on large-scale real-time RT-PCR. Mol Cancer 2004;3:20.
25. Bachelin C, Lachapelle F, Girard C, et al. Efficient myelin repair in the macaque spinal cord by autologous grafts of Schwann cells. Brain 2005;128: 540–9.
26. Rosenbaum T, Rosenbaum C, Winner U, Muller HW, Lenard HG, Hanemann CO. Long-term culture and characterization of human neurofibroma-derived Schwann cells. J Neurosci Res 2000;61:524–32.
27. Bieche I, Parfait B, Le Doussal V, et al. Identification of CGA as a novel estrogen receptor-responsive gene in breast cancer: an outstanding candidate marker to predict the response to endocrine therapy. Cancer Res 2001;61:1652–8.
28. Bieche I, Onody P, Laurendeau I, et al. Real-time reverse transcription-PCR assay for future management of ERBB2-based clinical applications. Clin Chem 1999;45:1148–56.
29. Ljubimov AV, Saghizadeh M, Spirin KS, et al. Expression of tenascin-C splice variants in normal and bullous keratopathy human corneas. Invest Ophthalmol Vis Sci 1998;39:1135–42.
30. Mann H, Whitney D. On a test of whether one of two random variables is stochastically larger than the other. Ann Math Stat 1947;18:50–60.
31. Hanley J, McNeil B. The meaning and use of the area under a receiver operating characteristic (ROC) curve. Radiology 1982;143:29–36.
32. D'Haene N, Maris C, Sandras F, et al. The differential expression of galectin-1 and galectin-3 in normal lymphoid tissue and non-Hodgkin's and Hodgkin's lymphomas. Int J Immunopathol Pharmacol 2005;18: 431–43.
33. Watson MA, Perry A, Tihan T, et al. Gene expression profiling reveals unique molecular subtypes of neurofibromatosis type I-associated and sporadic malignant peripheral nerve sheath tumors. Brain Pathol 2004;14: 297–303.
34. Miller SJ, Rangwala F, Williams J, et al. Large-scale molecular comparison of human Schwann cells to malignant peripheral nerve sheath tumor cell lines and tissues. Cancer Res 2006;66:2584–91.
35. Jones PL, Jones FS. Tenascin-C in development and disease: gene regulation and cell function. Matrix Biol 2000;19:581–96.
36. Chiquet-Ehrismann R. Tenascins. Int J Biochem Cell Biol 2004;36:986–90.
37. Joester A, Faissner A. The structure and function of tenascins in the nervous system. Matrix Biol 2001;20: 13–22.
38. Karube K, Nabeshima K, Ishiguro M, Harada M, Iwasaki H. cDNA microarray analysis of cancer associated gene expression profiles in malignant peripheral nerve sheath tumours. J Clin Pathol 2006;59:160–5.
39. Woodworth A, Pesheva P, Fiete D, Baenziger JU. Neuronal-specific synthesis and glycosylation of tenascin-R. J Biol Chem 2004;279:10413–21.
40. Geffrotin C, Horak V, Crechet F, et al. Opposite regulation of tenascin-C and tenascin-X in MeLiM swine heritable cutaneous malignant melanoma. Biochim Biophys Acta 2000;1524:196–202.
41. Burch GH, Gong Y, Liu W, et al. Tenascin-X deficiency is associated with Ehlers-Danlos syndrome. Nat Genet 1997;17:104–8.
42. Mao JR, Taylor G, Dean WB, et al. Tenascin-X deficiency mimics Ehlers-Danlos syndrome in mice through alteration of collagen deposition. Nat Genet 2002;30:421–5.
43. Matsumoto K, Takayama N, Ohnishi J, et al. Tumour invasion and metastasis are promoted in mice deficient in tenascin-X. Genes Cells 2001;6:1101–11.
44. Swindle CS, Tran KT, Johnson TD, et al. Epidermal growth factor (EGF)-like repeats of human tenascin-C as ligands for EGF receptor. J Cell Biol 2001;154: 459–68.
45. Ling BC, Wu J, Miller SJ, et al. Role for the epidermal growth factor receptor in neurofibromatosis-related peripheral nerve tumorigenesis. Cancer Cell 2005;7: 65–75.
46. D'haeseleer P, Liang S, Somogyi R. Genetic network inference: from co-expression clustering to reverse engineering. Bioinformatics 2000;16:707–26.
47. Nilsson M, Ford J, Bohm S, Toftgard R. Characterization of a nuclear factor that binds juxtaposed with ATF3/Jun on a composite response element specifically mediating induced transcription in response to an epidermal growth factor/Ras/Raf signaling pathway. Cell Growth Differ 1997;8:913–20.
48. Beiter K, Hiendlmeyer E, Brabletz T, et al. β-Catenin regulates the expression of tenascin-C in human colorectal tumors. Oncogene 2005;24:8200–4.
49. Jinnin M, Ihn H, Asano Y, Yamane K, Trojanowska M, Tamaki K. Tenascin-C upregulation by transforming growth factor-β in human dermal fibroblasts involves Smad3, Sp1, and Ets1. Oncogene 2004;23:1656–67.
50. Reardon DA, Akabani G, Coleman RE, et al. Phase II trial of murine (131)I-labeled antitenascin monoclonal antibody 81C6 administered into surgically created resection cavities of patients with newly diagnosed malignant gliomas. J Clin Oncol 2002;20:1389–97.
51. Rizzieri DA, Akabani G, Zalutsky MR, et al. Phase 1 trial study of ^{131}I-labeled chimeric 81C6 monoclonal antibody for the treatment of patients with non-Hodgkin lymphoma. Blood 2004;104:642–8.

Clinical Cancer Research

Microarray-Based Identification of *Tenascin C* and *Tenascin XB* , Genes Possibly Involved in Tumorigenesis Associated with Neurofibromatosis Type 1

Pascale Lévy, Hugues Ripoche, Ingrid Laurendeau, et al.

Clin Cancer Res 2007;13:398-407.